J Bioenerg Biomembr (2012) 44:607–614
DOI 10.1007/s10863-012-9461-0

Cataract-associated D3Y mutation of human connexin46 (hCx46) increases the dye coupling of gap junction channels and suppresses the voltage sensitivity of hemichannels

Barbara Schlingmann · Patrik Schadzek · Stefan Busko · Alexander Heisterkamp · Anaclet Ngezahayo

Received: 22 May 2012 / Accepted: 8 July 2012 / Published online: 28 July 2012

Abstract Connexin46 (Cx46), together with Cx50, forms gap junction channels between lens fibers and participates in the lens pump-leak system, which is essential for the homeostasis of this avascular organ. Mutations in Cx50 and Cx46 correlate with cataracts, but the functional relationship between the mutations and cataract formation is not always clear. Recently, it was found that a mutation at the third position of hCx46 that substituted an aspartic acid residue with a tyrosine residue (hCx46D3Y) caused an autosomal dominant zonular pulverulent cataract. We expressed EGFP-labeled hCx46wt and hCx46D3Y in HeLa cells and found that the mutation did not affect the formation of gap junction plaques. Dye transfer experiments using Lucifer Yellow (LY) and ethidium bromide (EthBr) showed an increased degree of dye coupling between the cell pairs expressing hCx46D3Y in comparison to the cell pairs expressing hCx46wt. In *Xenopus* oocytes, two-electrode voltage-clamp experiments revealed that hCx46wt formed voltage-sensitive hemichannels. This was not observed in the oocytes expressing hCx46D3Y. The replacement of the aspartic acid residue at the third position by another negatively charged residue, glutamic acid, to generate the mutant hCx46D3E, restored the voltage sensitivity of the resultant hemichannels. Moreover, HeLa cell pairs expressing hCx46D3E and hCx46wt showed a similar degree of dye coupling. These results indicate that the negatively charged aspartic acid residue at the third position of the N-terminus of hCx46 could be involved in the determination of the degree of metabolite cell-to-cell coupling and is essential for the voltage sensitivity of the hCx46 hemichannels.

Keywords hCx46 · N-terminus · Voltage sensitivity · Dye transfer · Hemichannels · Cataract

B. Schlingmann · P. Schadzek · S. Busko · A. Ngezahayo (✉)
Institute of Biophysics, Leibniz University Hannover,
Herrenhäuserstr. 2,
30419 Hannover, Germany
e-mail: ngezahayo@biophysik.uni-hannover.de

B. Schlingmann · A. Ngezahayo
Center for Systems Neuroscience Hannover,
University of Veterinary Medicine Hannover Foundation,
Buenteweg 2,
30559 Hannover, Germany

A. Heisterkamp
Institute of Applied Optics, Friedrich-Schiller-University-Jena,
Froebelstieg 1,
07743 Jena, Germany

Introduction

Connexins are transmembrane proteins that are encoded in humans by a gene family composed of 21 members (Sohl and Willecke 2004). In the membrane, all connexins adopt the same topology, with four transmembrane domains (TM) and two extracellular loops. Both the N- and C-terminus are localized in the cytoplasmic space, where a loop between TM2 and TM3 is also found (Falk et al. 1994). During trafficking to the cell membrane, connexins hexamerize and form the so-called connexons, or hemichannels. In the plasma membrane, the connexons of adjacent cells interact through the extracellular loops of the connexins and form gap junction channels, which are assembled in gap junction plaques that are found in the contact regions of adjacent cells. Gap junction channels allow the exchange of ions and metabolites between neighboring cells and are therefore essential for the formation of functional physiological units in tissue.

In the lens, three connexins, Cx43, Cx46 and Cx50, participate in the development and maturation of lens fibers (Gerido and White 2004; Goodenough 1992; White and Bruzzone 2000). Cx46 is mainly expressed in lens fibers,

where it forms, together with Cx50, gap junction channels, which are part of the pump-leak system that maintains the homeostasis of the lens (Donaldson et al. 2001; Mathias et al. 1997, 2010). The importance of gap junctions for lens physiology is attested by the malformations and cataract development that are correlated with mutations in both Cx50 and Cx46 (Berthoud and Beyer 2009); one such correlation was recently shown for an autosomal dominant zonular pulverulent cataract. This form of cataract was found to be related to a mutation in the N-terminus (NT) of hCx46, in which the aspartic acid residue at the third position was replaced by a tyrosine residue (hCx46D3Y) (Addison et al. 2006). To understand the relationship between the D3Y mutation and the development of the autosomal dominant zonular pulverulent cataract, the functional changes in the gap junction channels caused by the D3Y mutation must be studied.

Mutation of connexins can affect the formation of gap junctions at different levels. Some mutations affect connexin synthesis, connexin trafficking to the plasma membrane or docking of connexons in adjacent cells (Arora et al. 2006, 2008; Berthoud et al. 2003; Lichtenstein et al. 2009; Minogue et al. 2005; Thomas et al. 2008). Other mutations affect regulatory mechanisms, such as voltage-dependent gating (Minogue et al. 2009; Pal et al. 2000). For the voltage sensitivity, studies of Cx26 and Cx32 revealed that the six N-termini of a hemichannel lined the pore and contained charged amino acid residues that formed a part of the voltage sensor and are involved in ion permeation (Gonzalez et al. 2007; Maeda et al. 2009; Oh et al. 1999, 2000, 2004; Purnick et al. 2000a, b; Verselis et al. 1994). From analysis of the crystal structure, NMR and circular dichroism spectroscopy of Cx26 and Cx37, a structural model of the NT was proposed: residues 1–10 of Cx26 adopt a helical conformation, line the pore and form a funnel structure. The funnel structure is stabilized by a circular network of hydrogen bonds between the aspartic acid residue at the second position (D2) in one Cx-subunit and the threonine residue at the fifth position (T5) in the adjacent Cx-subunit (Maeda et al. 2009; Maeda and Tsukihara 2011). For Cx37, the residues between D3 and H16 may form a helical structure (Kyle et al. 2009). Further, a homology model predicted hydrogen bonds between the D3 of one subunit and both the phenylalanine at position six (F6) and the leucine at position seven (L7) of the adjacent subunit (Beyer et al. 2012). In the model for Cx26, the six N-termini form helices that move in an electrical field because of their charged residues. The movement of the N-termini can open or close the channel, depending on the direction of movement (Maeda and Tsukihara 2011).

For Cx46, it was shown that a replacement of the aspartic acid residue at the third position by an asparagine residue (D3N) changed the polarity of voltage gating in Cx46. Moreover, additional mutations in the NT of Cx46, such as D3A, D3C and D3G, altered the formation of functional hemichannels when expressed in oocytes (Srinivas et al. 2005). These findings provide evidence that D3 could be a part of the voltage sensor of Cx46.

In this report, HeLa cells and *Xenopus* oocytes were used as expression systems to compare the functional expression of the gap junction channels and the biophysical properties of hCx46wt and hCx46D3Y hemichannels. In HeLa cells, both hCx46wt and the mutant were equally expressed. LY and EthBr transfer experiments revealed that the degree of dye coupling was larger for cells expressing hCx46D3Y than for those expressing hCx46wt. In *Xenopus* oocytes, we found that the mutant hCx46D3Y did not form voltage-dependent hemichannels, indicating that the mutation induced a loss of the voltage-dependent regulation of the channels.

Materials and methods

Molecular biology

The pSP64TII vector that contained the hCx46 gene, which was kindly provided by Dr. Viviana Berthoud, was used as template for further cloning steps. For in vitro transcription, the hCx46 gene was inserted into the pGEMHE vector using *EcoR*I restriction sites (Walter et al. 2008). For the fluorescence imaging and dye transfer experiments, the hCx46 gene was PCR amplified and cloned into the pEGFP N1 vector (Clontech Laboratories, Mountain View, CA). The first two primers, which are described in Table 1, were used to generate *EcoR*I restriction sites, mutate the stop codon and fuse the gene in frame before EGFP with the addition of a 19-amino acid polylinker. The D3Y and D3E mutations were introduced by site-directed mutagenesis using the last six primers, which are described in Table 1. *Eschericha coli* XL10-Gold (Stratagene, Waldbronn Germany) was used to host the plasmids containing the different genes. All of the cloned vectors were verified by sequencing (Seqlab, Göttingen, Germany). The plasmid DNA for the transfection

Table 1 Primers used for the construction of expression vectors and for site-directed mutagenesis

Primer	5′-3′ sequence
pEGFP hCx46 fw	tccgaattcactagtgagccgccatgggcgactggag
pEGFP hCx46 rev	ctagagaattcgatttcctccgatggccaagtcctccgg
Mut D3Y pGEMHE fw	ctagtgatttgcaatgggctattggagctttctgggaagac
Mut D3Y pEGFP fw	tccgaattcactagtgagccgccatgggctattggag
Mut D3Y pGEMHE/ pEGFP rev	gtcttcccagaaagctccaatagcccattgcaaatcactag
Mut D3E pGEMHE fw	tagtgatttgcaatgggcgaatggagctttctgg
Mut D3E pGEMHE rev	ccagaaagctccattcgcccattgcaaatcacta
Mut D3E pEGFP fw	gagccgccatgggcgaatggagctttc
Mut D3E pEGFP rev	gaaagctccattcgcccatggcggctc

experiments was purified using the QIAprep Spin Miniprep Kit (QIAGEN, Hilden, Germany). For in vitro transcription, the coding region, including the T7 promotor, was amplified and purified using a PCR purification kit (QIAGEN, Hilden, Germany). The cRNA of the different hCx46 variants was prepared using a synthesis kit containing T7 RNA polymerase and CAP analogue, which was purchased from Ambion (Austin, USA). The transcript concentration was estimated spectrophotometrically and analyzed on agarose gels.

Expression in HeLa cells

HeLa cells were cultivated using Dulbecco´s Modified Eagle´s Medium (DMEM/Ham's F12, 1:1) (Biochrom, Berlin, Germany) supplemented with 10 % fetal calf serum (FCS) (PAA, Pasching, Austria), penicillin and streptomycin (100 U/ml and 10 mg/ml, respectively). The cultures were maintained at 37 °C in a humidified atmosphere containing 5 % CO_2.

For the transfection experiments, cover slips (Ø 10 mm) coated with rat collagen I (150 μg/ml) (Cultrex, Gaithersburg USA) were placed into a 24-multiwell plate. 7×10^4 cells/well were seeded. OptiMEM® (Gibco, Invitrogen) containing 0.5 μg plasmid DNA and 1.5 μl FuGENE HD Transfection reagent (Roche, Penzberg, Germany) was used. The examination of gap junction plaque formation and the dye transfer experiments were performed 24–48 h after transfection. For each hCx46 variant, cells of at least three different passages were transfected. For all of the transfected hCx46 variants, the transfection efficiency was between 50 and 70 %.

Formation of gap junction plaques

The fluorescence images were acquired using an inverted Nikon Eclipse TE2000-E confocal laser scanning microscope with a 60× water immersion objective (Nikon, Düsseldorf, Germany). The EZ-C1 3.80 software (Nikon, Düsseldorf, Germany) was used to record the images. During the different experiments, the settings for gain, brightness, contrast, and pixel dwell time remained constant. The images were taken at a resolution of 2048×2048 pixels. To improve cell selection, the nuclei of the transfected cells were stained with Hoechst 33342 (1 μg/ml) (Sigma Aldrich) and the cell membranes were stained with Wheat Germ Agglutinin Alexa555 (5 μg/ml) (Molecular Probes, Eugene, OR, USA). The cells were fixed with 3.7 % formaldehyde. To quantify the plaque formation of the hCx46 variants, the expressing cell pairs were counted in a double-blind randomized fashion. The plaque formation was quantified using ImageJ (http://rsbweb.nih.gov/ij/docs/menus/analyze.html#plot). For each transfection, five cover slips were evaluated. Four images from different sections of a cover slip were taken. For each construct, the average ratio of the number of cell pairs that formed gap junction plaques to the total number of cell pairs expressing the corresponding construct is given. The error bars are the SEM, and the statistical significance of changes was evaluated by Student's *t*-test (** for $p\leq0.01$ and * for $p\leq0.05$).

Functional formation of gap junction channels of the hCx46 variants

Formation of functional gap junction channels was evaluated using dye transfer experiments. Cover slips with transfected cells were transferred to a perfusion chamber containing 500 μl of a bath solution composed of (in mM) 121 NaCl, 5.4 KCl, 6 $NaHCO_3$, 5.5 glucose, 0.8 $MgCl_2$, 1.6 $CaCl_2$, and 25 HEPES at pH 7.4 and mounted on a Zeiss inverted fluorescence microscope (Oberkochen, Germany). For the dye transfer experiments, a whole-cell patch-clamp configuration was established on a cell of a pair expressing the EGFP-labeled hCx46 variant using a EPC7 patch-clamp amplifier (List Medical, Darmstadt, Germany). Lucifer Yellow lithium salt (LY) (1 mg/ml) (Biotium, Hayward CA) or ethidium bromide (EthBr) (1 mg/ml) (Sigma Aldrich) was diluted in a pipette medium containing (in mM) 135 K-Gluconate, 5 KCl, 10 HEPES, 1 $MgCl_2$, 1 $CaCl_2$, 2 glucose, 5 Na_2ATP, 5 EGTA, 0.1 cAMP, 0.1 cGMP at pH 7.4. A Polychrome II monochromator (T.I.L.L. Photonics GmbH, Planegg, Germany) equipped with a 75 W XBO xenon lamp was used to excite the fluorescent molecules (EGFP-labeled hCx46 variant at 488 nm, LY at 410 nm and EthBr at 350 nm). The images were taken with a digital CCD camera (C4742-95, Hamamatsu Photonics K.K.; Japan) using Aquacosmos software (Hamamatsu Photonics K.K.; Japan). For each variant, the degree of dye coupling was estimated as the ratio of the number of coupled pairs to the total number of tested pairs expressing the particular variant. The results are given as the average values. The error bars represent the SEM. The significance of the difference was evaluated by Student's *t*-test (** for $p\leq0.01$ and * for $p\leq0.05$).

Expression of hCx46 in *Xenopus* oocytes

The expression of the hCx46 variants in *Xenopus* oocytes was performed as previously described (Walter et al. 2008). Follicles containing oocytes were harvested form anesthetized frog. The oocytes were isolated by a treatment of the follicles with collagenase type II in modified Barth medium without Ca^{2+} (mM: 88 NaCl, 1 KCl, 0.82 $MgCl_2\times6\ H_20$, 5 glucose, 2.4 $NaHCO_3$, 15 Hepes at pH 7.4). The oocytes were injected with 23 nl of cRNA solution (1 μg/μl) and the antisense to the endogenous Cx38 (400 ng/μl). The antisense DNA (AS38) with the sequence C*T*GACTGCTCGTCTGTCCACAC*A*G*

```
      Y/E
  1 MGDWSFLGRL LENAQEHSTV IGKVWLTVLF IFRILVLGAA AEDVWGDEQS
                                  TM 1
 51 DFTCNTQQPG CENVCYDRAF PISHIRFWAL QIIFVSTPTL IYLGHVLHIV
                                        TM 2
101 RMEEKKKERE EEEQLKRESP SPKEPPQDNP SSRDDRGRVR MAGALLRTYV
151 FNIIFKTLFE VGFIAGQYFL YGFELKPLYR CDRWPCPNTV DCFISRPTEK
          TM 3
201 TIFIIFMLAV ACASLLLNML EIYHLGWKKL KQGVTSRLGP DASEAPLGTA
              TM 4
251 DPPPLPPSSR PPAVAIGFPP YYAHTAAPLG QARAVGYPGA PPPAADFKLL
301 ALTEARGKGQ SAKLYNGHHH LLMTEQNWAN QAAERQPPAL KAYPAASTPA
351 APSPVGSSSP PLAHEAEAGA APLLLDGSGS SLEGSALAGT PEEEEQAVTT
401 AAQMHQPPLP LGDPGRASKA SRASSGRARP EDLAI
```

Fig. 1 Amino acid sequence of hCx46. The transmembrane domains, as predicted by TMHMM software (version 2.0), are underlined (Hansen et al. 2006; Krogh et al. 2001). The mutations introduced by site-directed mutagenesis are indicated as bold letters above the respective amino acid

(* indicates phosphothioate modifications) was purchased from Eurofins MWG Operon (Ebersberg, Germany). For the control experiments, 23 nl of AS38 (400 ng/μl) was injected. For expression, the injected oocytes were incubated for at least 12 h at 18 °C in modified Barth medium containing 2.4 mM $CaCl_2$.

Electrophysiological measurements

The recordings of the macroscopic currents with two-electrode voltage-clamp technique were performed on single *Xenopus* oocytes 12–36 h after cRNA injection. The oocytes were transferred into a perfusion chamber containing nominal Ca^{2+}-free modified Barth solution at room temperature. From a constant holding voltage of -90 mV, test voltage pulses ranging from -100 mV to +30 mV were applied for 3 s in 10 mV steps. The voltage-evoked currents were filtered at 1 kHz and sampled at 5 kHz. The data acquisition and analysis were performed as previously described (Walter et al. 2008). For the steady-state current voltage plots (I(V)), the amplitude of the steady-state currents at the end of each voltage pulse was measured and plotted against the corresponding voltage. To estimate the activation parameters of the connexons, the macroscopic conductance for the different voltage pulses was calculated and plotted against the corresponding voltages in a G(V) plot. The data points were fitted with a simple Boltzmann equation, as previously described (Walter et al. 2008).

Results

Recently, it was shown that a mutation in the human connexin46 that changed the third amino acid residue in the NT from the negatively charged aspartic acid to the neutral tyrosine correlates with cataract (Addison et al. 2006). We used recombinant systems to investigate the functional consequences of this mutation. To test whether the D3Y mutation suppressed the ability of connexins to form gap junction channels, plasmids encoding EGFP-labeled hCx46wt and hCx46D3Y were transfected into HeLa cells. Confocal microscopy imaging followed by gap junction plaque counting revealed that both connexin variants were transported to the membrane and formed gap junction

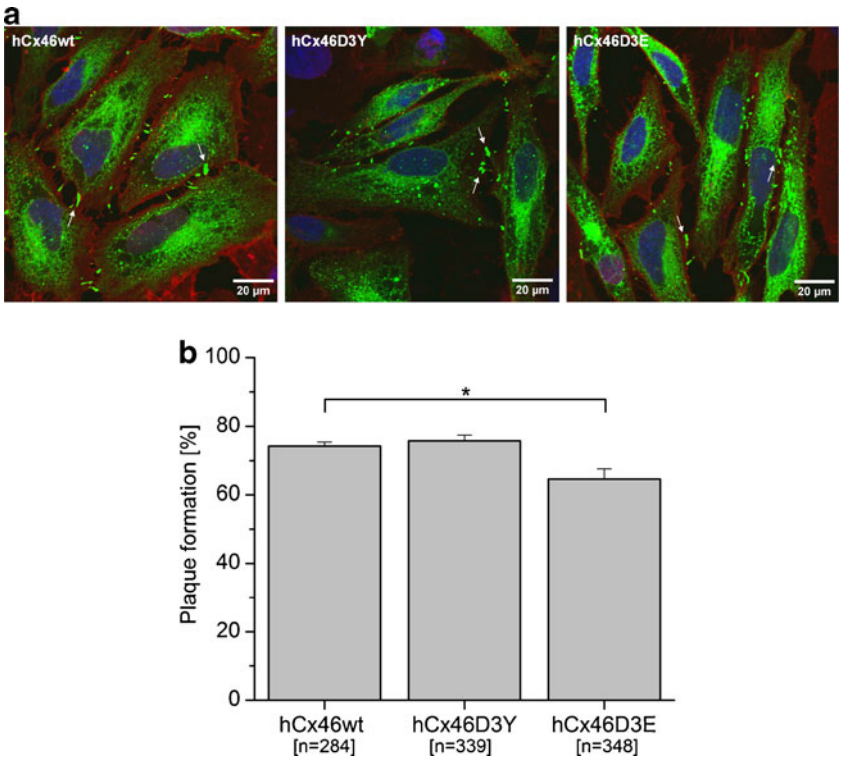

Fig. 2 hCx46 gap junction formation in HeLa cells. The cells were transfected with different hCx46-EGFP variants. After 24 h expression time, the cell nuclei were stained with Hoechst. The cells were fixed with 3.7 % formaldehyde, and the membranes were stained with WGA conjugated to Alexa Fluor 555. (**a**) Representative images of each hCx46 variant are shown. The arrows indicate gap junction plaques. (**b**) Quantification of plaque formation; the percentage of cell pairs with gap junction plaques to all cell pairs expressing a hCx46 variant is given. For each variant, at least five transfection experiments were performed. The results are given as the average. The error bars represent the SEM. The significance of the difference was evaluated by Student's *t*-test (** $p \leq 0.01$; * $p \leq 0.05$)

plaques (Fig. 1, Fig. 2). Gap junction plaques were found in 74.3 % ±1.2 and 75.8 % ±1.7 of all of the transfected cell pairs expressing hCx46wt and hCx46D3Y, respectively.

To determine whether the gap junction plaques contained functional gap junction channels, we performed dye transfer experiments using LY, a negatively charged (-2) 443 Da molecule, and EthBr, a positively charged (+1) 314 Da molecule, as tracers (Elfgang et al. 1995; Abbaci et al. 2008). Both the wild type and the mutant formed functional gap junction channels. Of all tested cell pairs expressing hCx46wt, 35.2 % ±3.3 were able to transfer LY, whereas cell pairs expressing hCx46D3Y showed a significantly increased ability to transfer LY (62.5 %±12.5) (Fig. 3). The dye coupling experiments with EthBr gave comparable results (hCx46wt 29.2 %±2.4, hCx46D3Y 53 %±8.3). Quantification of the plaque formation and size (data not shown) revealed no significant differences in the ability of hCx46wt and hCx46D3Y to form gap junction plaques (Fig. 2). The increase in gap junction coupling in cells expressing EGFP-labeled hCx46D3Y was not caused by a higher density of gap junction channels in the membrane (Fig. 2, Fig. 3).

Connexins of the Cx46-class can form voltage-dependent gap junction hemichannels when expressed in *Xenopus* oocytes (Ebihara et al. 1995; Pal et al. 2000; Paul et al. 1991; Walter et al. 2008). We therefore expressed both hCx46wt and hCx46D3Y in *Xenopus* oocytes. The hemichannels that were formed were analyzed with the two-electrode-voltage clamp technique. In oocytes expressing hCx46wt, a voltage-dependent current was found (Fig. 4). The currents were induced by depolarizing voltages above

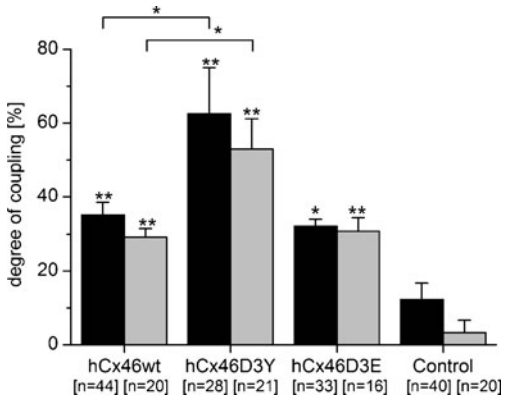

Fig. 3 Dye coupling experiments. A whole-cell patch-clamp configuration was established with a LY- (1 mg/ml) (black bar) or EthBr- (1 mg/ml) (grey bar) containing pipette-filling solution onto one cell of a HeLa cell pair expressing EGFP-labeled hCx46 variants. The degree of dye coupling was estimated as the ratio of the sum of the coupled pairs to the sum of the tested pairs. For each hCx46 variant, at least four transfection experiments were performed. The results are given as the average. The error bars represent the SEM. The significance of the difference between the control (non transfected HeLa cells) and the respectively hCx46 variant was evaluated by Student's *t*-test ** $p \leq 0.01$; * $p \leq 0.05$. The significance of the difference between hCx46wt and the respectively mutant are indicated by underlined stars

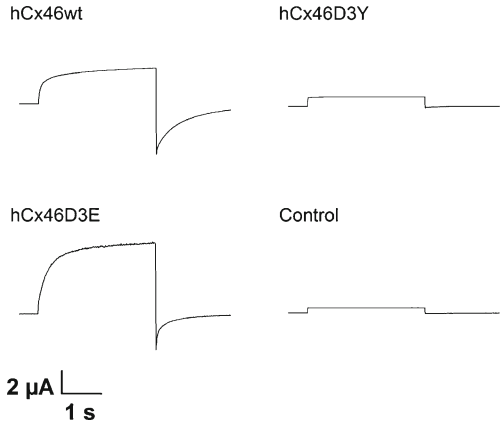

Fig. 4 Representative current evoked in oocytes expressing the different hCx46 variants. From a holding potential of -90 mV, the oocytes were depolarized to 30 mV. The oocytes were injected with the indicated hCx46 variant and AS38. The expression time was 12 h. The control oocytes were only injected with the AS38

-60 mV (Fig. 5). The voltage dependence of the currents is also shown in the steady-state current-voltage plot (I(V)). The fitting of the voltage-conductance G(V) plot for hCx46wt to a Boltzmann equation (Fig. 6) revealed a half activation voltage ($V_{1/2}$) of -24.02 mV±4.89 and an apparent gating charge *z* of 1.85±0.17 (Table 2). In the oocytes expressing hCx46D3Y hemichannels, a voltage-dependent current was not observed (Fig. 4, Fig. 5). The currents observed in oocytes expressing the hCx46D3Y mutant are comparable to those observed in the control oocytes. This result indicates that, although hCx46D3Y was inserted into the plasma membrane and formed functional gap junction channels when expressed in HeLa cells (Fig. 2, Fig. 3), it was not able to form voltage-sensitive hemichannels when expressed in *Xenopus* oocytes (Fig. 4, Fig. 5).

The D3Y mutation replaces a negatively charged residue with a neutral amino acid residue at the third position (Fig. 1) and impairs the formation of voltage-dependent

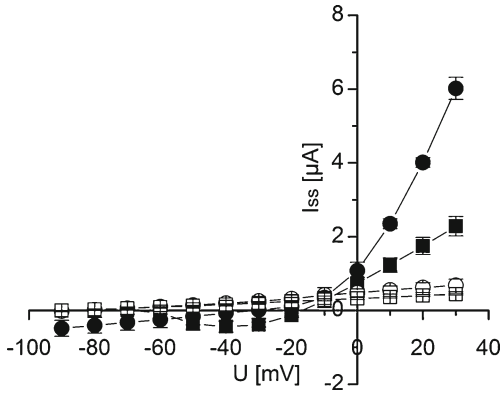

Fig. 5 I(V) plots obtained from oocytes expressing hemichannels composed of hCx46wt (■), hCx46D3Y (○), and hCx46D3E (●), and from control oocytes (□). The results are given as the average of at least five different oocytes for each variant. The error bars represent the SEM

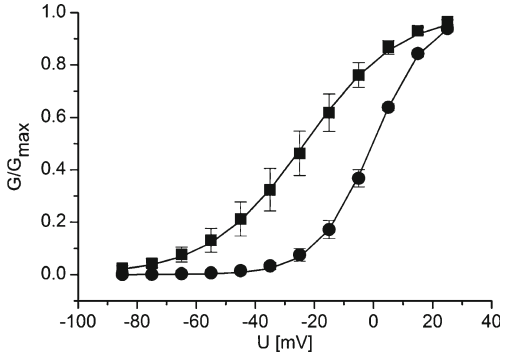

Fig. 6 G(V) plots obtained from oocytes expressing hemichannels of hCx46wt (■) and hCx46D3E (●). For each experiment, the conductance was normalized to the maximum conductance for hCx46wt and hCx46D3E as appropriate. The data points are the averages of the normalized values obtained from at least five experiments for each variant. The error bars are the SEM. The curves represent the fitting of the data points to the Boltzmann equation

hemichannels (Fig. 4, Fig. 5). Therefore, we speculated that a reintroduction of a negative charge at the same position would restore the voltage sensitivity. Using site-directed mutagenesis, we introduced the negatively charged glutamic acid (D3E), instead of tyrosine or aspartic acid, to the third position. Two-electrode voltage-clamp measurements revealed that like hCx46wt, hCx46D3E expressed in *Xenopus* oocytes formed voltage-dependent hemichannels (Fig. 4, Fig. 5), despite some differences, such as a high macroscopic conductance (Fig. 5) and a shift of $V_{1/2}$ by approximately 23 mV to -0.53 mV ±0.92 compared with hCx46wt (Table 2, Fig. 6). HeLa cells pairs expressing hCx46D3E, which was labeled with EGFP showed a reduced formation of gap junction plaques (63.6 % ±2.6) compared with cell pairs expressing hCx46wt (74.3 % ±1.2). From the dye coupling experiments, however, a similar degree of LY and EthBr transfer between cells pairs forming hCx46D3E gap junction plaques (LY: 32.2 % ±1.8, EthBr: 30.9 % ±3.6) and cell pairs forming hCx46wt gap junction plaques (LY: 35.2 % ±3.3, EthBr: 29.2 % ±4.8) was found (Fig. 3).

In summary, the results described above show that the replacement of aspartic acid, a negatively charged residue, with tyrosine, a neutral residue, at the third position of the Cx46 NT did not affect the synthesis and hexamerization of the connexins or the trafficking and insertion of the connexons into the plasma membrane. Compared to the wild type, the D3Y mutation correlated with an increased degree of dye transfer between the cells and a suppression of the voltage sensitivity for hemichannels expressed in *Xenopus* oocytes.

Table 2 Activation parameter as estimated by fitting the G(V) data points of different experiments with the Boltzmann equation. The data are given as the averages ±SEM for at least n=5 oocytes for each connexin variant

connexin	$V_{1/2}$ [mV]	z
hCx46wt	-24.02 ±4.87	1.85±0.17
hCx46D3E	-0.53 ±0.92	0.43±0.27

Discussion

The present report examines how the exchange of the third amino acid residue from a negatively charged aspartic acid residue to a neutral tyrosine residue (D3Y) in hCx46, which causes an autosomal dominant zonular pulverulent cataract (Addison et al. 2006), affects gap junction formation and functionality. Confocal microscopy analysis of HeLa cells expressing EGFP-labeled hCx46wt and hCx46D3Y did not reveal any difference in the expression level and in the formation of gap junction plaques between the two hCx46 variants (Fig. 2). It is noteworthy that the transfection efficiency for both hCx46wt and hCx46D3Y varied between 50 % and 70 %. Plaque counting shows that the trafficking of the protein is not affected by the D3Y mutation (Fig. 2). The mutated hCx46D3Y protein is synthesized, transported and inserted into the plasma membrane in a comparable manner and with a similar intensity to the wild type hCx46. This finding is in agreement with the observation published by other authors which shows that mutations in the NT and even deletion of as much as half of the NT of hCx37 did not affect the transport of the proteins and their capacity to form gap junction plaques (Kyle et al. 2008).

We also tested whether the formed gap junction plaques were functional. LY and EthBr transfer experiments revealed that the D3Y mutation correlated with an increased degree of dye coupling (LY: 62.5 % ±12.5, EthBr: 53 % ±8.3) compared with the wild type (Fig. 3). This increase appears to be related to the negative charge of the aspartic acid residue at the third position because a similar ability to transfer LY and EthBr through gap junction channels was found in HeLa cells expressing hCx46wt (LY: 35.2 ±3.3, EthBr: 29.2 % ±2.4) and HeLa cells expressing our generated mutant hCx46D3E (LY: 32.2 % ±1.8, EthBr: 30.9 % ±3.6). Different scenarios can be proposed to explain the results observed in the dye transfer experiments for these hCx46 variants. (a) Within a gap junction plaque composed of hCx46D3Y, more hemichannels dock to each other and form open functional gap junction channels between adjacent cells. (b) Due to the loss of the negative charge at the third position, the single-channel permeability to LY and EthBr of gap junction channels composed of hCx46D3Y is increased compared with the single-channel permeability of gap junction channels composed of hCx46wt or hCx46D3E. Whether mutations in the NT of connexins could affect the docking of hemichannels in adjacent cells is not yet known. In contrast, it is known that the N-termini of the six

connexins that form a connexon line the pore entrance and form a funnel, which might be critical for the opening and determination of permeability of gap junction channels (Dong et al. 2006; Kyle et al. 2009; Maeda et al. 2009; Purnick et al. 2000a). For Cx26, the N-termini of the six connexins line the pore entrance and form a funnel, which is stabilized by hydrogen bonds between the aspartic acid residue at the second position (D2) in one Cx-subunit and the threonine residue at the fifth position (T5) in the adjacent Cx-subunit (Beyer et al. 2012; Maeda et al. 2009). In a homology model of Cx37, an interaction of D3 with F6 and L7 similar to the corresponding interaction in Cx26 is predicted (Beyer et al. 2012). Despite minor differences in the amino acid sequences of the Cx37 NT and Cx46 NT, an organization of the N-termini in a structure comparable to the funnel proposed for the N-termini of Cx37 can be assumed. In this structure, the D3 residue plays a key role in the electrostatic organization of the N-termini. The replacement of a charged residue (D3) with a neutral residue (Y) could affect the electrostatic stability of the funnel and the permeability of the channels, which would lead to the results presented in this report (Fig. 3). In addition to forming the funnel, the N-termini line the pore of the channels and serve as a voltage sensor that contains charged amino acid residues, which are important for the rapid voltage gating (Gonzalez et al. 2007; Maeda et al. 2009; Oh et al. 1999, 2000, 2004; Purnick et al. 2000a, b; Verselis et al. 1994). For Cx46, it was shown that the NT had a crucial role in voltage-dependent gating (Tong et al. 2004). It was also found that a replacement of the aspartic acid residue by an asparagine residue at the third position affected the voltage gating of Cx46 gap junction channels (Srinivas et al. 2005). Therefore, it can be hypothesized that the D3Y mutation, which replaces a negatively charged residue with a neutral residue, would affect the voltage sensitivity of hCx46 channels. This hypothesis is verified by the two-electrode voltage-clamp experiments, which show that the depolarization of *Xenopus* oocytes expressing hCx46wt hemichannels activated a current that was not observed in oocytes expressing hCx46D3Y hemichannels (Fig. 4, Fig. 5). These results indicate that the D3Y mutation correlated with a loss of voltage sensitivity. Furthermore, the observation that ooyctes expressing hCx46D3E formed voltage-activated hemichannels (Fig. 4, Fig. 5), emphasizes the crucial role of the charged residue at the third position in the NT for the voltage sensitivity of hCx46**.** The mechanism by which this charged residue controls the voltage gating of hCx46 is not understood so far. For Cx26, residues 1–10 of the connexins are organized in helices that can move within a transjunctional voltage field, leading to opening or closing of the channel vestibule (Maeda and Tsukihara 2011; Purnick et al. 2000a)**.** For Cx37, a possibility to form a helical structure between residues 3–16 was proposed (Kyle et al. 2009). The NT of hCx46 is not completely similar to the NT of Cx26 and Cx37. However, as proposed by other authors (Beyer et al. 2012; Maeda and Tsukihara 2011; Srinivas et al. 2005), it could be assumed that the hCx46 N-termini may adopt helical structures with the aspartic acid residues facing the cytoplasmic space. Because of the charged aspartic acid residues, the N-termini could move in the voltage field, leading to channel opening or closing (Maeda and Tsukihara 2011). Structure analysis using NMR spectroscopy or crystal structure analysis, which we cannot offer, should be performed to clarify the structure of the hCx46 NT. On the basis of our results, we propose that the replacement of a negatively charged residue with a neutral residue at the third position in the NT of hCx46 suppresses a regulatory mechanism of the resultant channels.

Conclusion

The present report shows that the hCx46D3Y mutation, which correlates with a cataract, did not change the functional expression of hCx46. Dye transfer experiments revealed an increased degree of coupling for cells expressing hCx46D3Y compared with cell pairs expressing hCx46wt. A replacement of the aspartic acid residue at third position by a glutamic acid residue, which is also negatively charged, showed a reduced formation of gap junction plaques, but the degree of coupling was similar for cells expressing hCx46D3E and hCx46wt. Thus, the negatively charged residue at the third position could be involved in the docking of functional gap junction channels and/or the modulation of the permeability of hCx46 channels. Additionally, we show that the negatively charged aspartic acid residue at the third position is essential for correct voltage sensitivity of hCx46 gap junction hemichannels and most likely also for the gap junction channels. The loss of voltage sensitivity is a loss of a regulatory mechanism, which, in turn, could impair the function of gap junction channels in the lens, leading to cataract formation.

Acknowledgements This work was supported by Transregio TR37. We thank Viviane Berthoud for the hCx46 clone.

References

Abbaci M, Barberi-Heyob M, Blondel W, Guillemin F, Didelon J (2008) Advantages and limitations of commonly used methods to assay the molecular permeability of gap junctional intercellular communication. Biotechniques 45:33–62

Addison PK, Berry V, Holden KR, Espinal D, Rivera B, Su H, Srivastava AK, Bhattacharya SS (2006) A novel mutation in the connexin 46 gene (GJA3) causes autosomal dominant zonular pulverulent cataract in a Hispanic family. Mol Vis 12:791–795

Arora A, Minogue PJ, Liu X, Addison PK, Russel-Eggitt I, Webster AR, Hunt DM, Ebihara L, Beyer EC, Berthoud VM, Moore AT

(2008) A novel connexin50 mutation associated with congenital nuclear pulverulent cataracts. J Med Genet 45:155–160

Arora, A., Minogue, P.J., Liu, X., Reddy, M.A., Ainsworth, J.R., Bhattacharya, S.S., Webster, A.R., Hunt, D.M., Ebihara, L., Moore, A.T., Beyer, E.C. and Berthoud, V.M. (2006) A novel GJA8 mutation is associated with autosomal dominant lamellar pulverulent cataract: further evidence for gap junction dysfunction in human cataract. J Med Genet. 43:e2 (http://www.jmedgenet.com/cgi/content/full/43/1/e2)

Berthoud VM, Beyer EC (2009) Oxidative stress, lens gap junctions, and cataracts. Antioxid Redox Signal 11:339–353

Berthoud VM, Minogue PJ, Guo J, Williamson EK, Xu X, Ebihara L, Beyer EC (2003) Loss of function and impaired degradation of a cataract-associated mutant connexin50. Eur J Cell Biol 82:209–221

Beyer EC, Lipkind GM, Kyle JW, Berthoud VM (2012) Structural organization of intercellular channels II. Amino terminal domain of the connexins: sequence, functional roles, and structure. Biochim Biophys Acta 1818:1823–1830

Donaldson P, Kistler J, Mathias RT (2001) Molecular solutions to mammalian lens transparency. News Physiol Sci 16:118–123

Dong L, Liu X, Li H, Vertel BM, Ebihara L (2006) Role of the N-terminus in permeability of chicken connexin45.6 gap junctional channels. J Physiol 576:787–799

Ebihara, L., Berthoud, V.M. and Beyer, E.C. (1995) Distinct behavior of connexin56 and connexin46 gap junctional channels can be predicted from the behavior of their hemi-gap-junctional channels. Biophys J.68:1796-1803

Elfgang C, Eckert R, Lichtenberg-Frate H, Butterweck A, Traub O, Klein RA, Hulser DF, Willecke K (1995) Specific permeability and selective formation of gap junction channels in connexin-transfected HeLa cells. J Cell Biol 129:805–817

Falk MM, Kumar NM, Gilula NB (1994) Membrane insertion of gap junction connexins: polytopic channel forming membrane proteins. J Cell Biol 127:343–355

Gerido DA, White TW (2004) Connexin disorders of the ear, skin, and lens. Biochim Biophys Acta 1662:159–170

Gonzalez D, Gomez-Hernandez JM, Barrio LC (2007) Molecular basis of voltage dependence of connexin channels: an integrative appraisal. Prog Biophys Mol Biol 94:66–106

Goodenough DA (1992) The crystalline lens. A system networked by gap junctional intercellular communication. Semin Cell Biol 3:49–58

Hansen L, Yao W, Eiberg H, Funding M, Riise R, Kjaer KW, Hejtmancik JF, Rosenberg T (2006) The congenital "ant-egg" cataract phenotype is caused by a missense mutation in connexin46. Mol Vis 12:1033–1039

Krogh A, Larsson B, von Heijne G, Sonnhammer EL (2001) Predicting transmembrane protein topology with a hidden Markov model: application to complete genomes. J Mol Biol 305:567–580

Kyle JW, Berthoud VM, Kurutz J, Minogue PJ, Greenspan M, Hanck DA, Beyer EC (2009) The N terminus of connexin37 contains an alpha-helix that is required for channel function. J Biol Chem 284:20418–20427

Kyle JW, Minogue PJ, Thomas BC, Domowicz DA, Berthoud VM, Hanck DA, Beyer EC (2008) An intact connexin N-terminus is required for function but not gap junction formation. J Cell Sci 121:2744–2750

Lichtenstein A, Gaietta GM, Deerinck TJ, Crum J, Sosinsky GE, Beyer EC, Berthoud VM (2009) The cytoplasmic accumulations of the cataract-associated mutant, Connexin50P88S, are long-lived and form in the endoplasmic reticulum. Exp Eye Res 88:600–609

Maeda S, Nakagawa S, Suga M, Yamashita E, Oshima A, Fujiyoshi Y, Tsukihara T (2009) Structure of the connexin 26 gap junction channel at 3.5 A resolution. Nature 458:597–602

Maeda S, Tsukihara T (2011) Structure of the gap junction channel and its implications for its biological functions. Cell Mol Life Sci 68:1115–1129

Mathias RT, Rae JL, Baldo GJ (1997) Physiological properties of the normal lens. Physiol Rev 77:21–50

Mathias RT, White TW, Gong X (2010) Lens gap junctions in growth, differentiation, and homeostasis. Physiol Rev 90:179–206

Minogue PJ, Liu X, Ebihara L, Beyer EC, Berthoud VM (2005) An aberrant sequence in a connexin46 mutant underlies congenital cataracts. J Biol Chem 280:40788–40795

Minogue PJ, Tong JJ, Arora A, Russell-Eggitt I, Hunt DM, Moore AT, Ebihara L, Beyer EC, Berthoud VM (2009) A mutant connexin50 with enhanced hemichannel function leads to cell death. Invest Ophthalmol Vis Sci 50:5837–5845

Oh S, Abrams CK, Verselis VK, Bargiello TA (2000) Stoichiometry of transjunctional voltage-gating polarity reversal by a negative charge substitution in the amino terminus of a connexin32 chimera. J Gen Physiol 116:13–31

Oh S, Rivkin S, Tang Q, Verselis VK, Bargiello TA (2004) Determinants of gating polarity of a connexin 32 hemichannel. Biophys J 87:912–928

Oh S, Rubin JB, Bennett MV, Verselis VK, Bargiello TA (1999) Molecular determinants of electrical rectification of single channel conductance in gap junctions formed by connexins 26 and 32. J Gen Physiol 114:339–364

Pal JD, Liu X, Mackay D, Shiels A, Berthoud VM, Beyer EC, Ebihara L (2000) Connexin46 mutations linked to congenital cataract show loss of gap junction channel function. Am J Physiol Cell Physiol 279:C596–C602

Paul DL, Ebihara L, Takemoto LJ, Swenson KI, Goodenough DA (1991) Connexin46, a novel lens gap junction protein, induces voltage-gated currents in nonjunctional plasma membrane of Xenopus oocytes. J Cell Biol 115:1077–1089

Purnick PE, Benjamin DC, Verselis VK, Bargiello TA, Dowd TL (2000a) Structure of the amino terminus of a gap junction protein. Arch Biochem Biophys 381:181–190

Purnick PE, Oh S, Abrams CK, Verselis VK, Bargiello TA (2000b) Reversal of the gating polarity of gap junctions by negative charge substitutions in the N-terminus of connexin 32. Biophys J 79:2403–2415

Sohl G, Willecke K (2004) Gap junctions and the connexin protein family. Cardiovasc Res 62:228–232

Srinivas M, Kronengold J, Bukauskas FF, Bargiello TA, Verselis VK (2005) Correlative studies of gating in Cx46 and Cx50 hemichannels and gap junction channels. Biophys J 88:1725–1739

Thomas BC, Minogue PJ, Valiunas V, Kanaporis G, Brink PR, Berthoud VM, Beyer EC (2008) Cataracts are caused by alterations of a critical N-terminal positive charge in connexin50. Invest Ophthalmol Vis Sci 49:2549–2556

Tong JJ, Liu X, Dong L, Ebihara L (2004) Exchange of gating properties between rat cx46 and chicken cx45.6. Biophys J 87:2397–2406

Verselis VK, Ginter CS, Bargiello TA (1994) Opposite voltage gating polarities of two closely related connexins. Nature 368:348–351

Walter WJ, Zeilinger C, Bintig W, Kolb HA, Ngezahayo A (2008) Phosphorylation in the C-terminus of the rat connexin46 (rCx46) and regulation of the conducting activity of the formed connexons. J Bioenerg Biomembr 40:397–405

White TW, Bruzzone R (2000) Intercellular communication in the eye: clarifying the need for connexin diversity. Brain Res Brain Res Rev 32:130–137